Supplementary Information

Self-assembly of block copolymer-based ionic supramolecules based upon multi-tail amphiphiles

M. Asad Ayoubi,*[a] K. Almdal,[b] K. Zhu,[c] B. Nyström,[c] U. Olsson,[a] and L. Piculell[a]

[a] Division of Physical Chemistry, Center for Chemistry and Chemical Engineering, Lund University, SE-22 100 Lund, Sweden.
[b] Department of Micro- and nanotechnology, Technical University of Denmark, DTU Nanotech, Building 423, DK-2800 Kongens Lyngby, Denmark.
[c] Department of Chemistry, University of Oslo, P.O. Box 1033, Blindern, N-0315 Oslo, Norway.

1. Form-factor simulation of a cylinder

Form factor of a cylinder $P(q)$ is[1]

$$P(q,R,L)=\int_0^{\frac{\pi}{2}} f^2(q,\beta)\sin\beta d\beta$$
$$f(q,\beta)=8\pi R^2 L j_0\left(\frac{qL'}{2}\beta\right)\frac{j_1(qR\sin\beta)}{qR\sin\beta} \qquad \text{(SI-1)}$$

, where $j_0(x)=\sin x/x$, $j_1(x)$ is the first order Bessel function, R is the radius of the cylinder, L is its length and β is the angle between the cylinder axis and the q-vector. Thus, in eqn. SI-1 the cylinder form factor is an average over all possible orientations of the cylinder with respect to the q-vector. We have used Irena SAXS analysis package[2] that has implemented the code for $P(q)$. The results are shown in Figure 3, c-e, of the paper.

2. SAXS modeling of SPH$_{LL}$ microdomains

The scattering intensity $I(q)$ of a collection of spheres (which in our case represent the micro-segregated AC-block domains) is compared to the experimental scattering pattern and the characteristics of the system is determined as extracted fitting parameters. The intensity is related to intra-particle (i.e. form-factor) scattering $P'(q)$ and inter-particle (i.e. structure factor) scattering $S(q)$ in the following manner:[3]

$$I(q)\sim P'(q)S(q) \qquad \text{(SI-2)}$$

$P'(q)$ for a system of spheres (radius R) is

$$P'(q,R)=(\frac{4}{3}\pi R^3)^2\left(\frac{3[\sin(qR)-qR\cos(qR)]}{(qR)^3}\right)^2 \qquad \text{(SI-3)}$$

In order to account for polydispersity in size of spheres we convolute $P'(q,R)$ with a Gaussian function $p(R)$ with a standard deviation of κ. Thus we have

$$P'(q,\bar{R},\kappa)=\frac{\int_0^\infty P'(q,R)p(R)dR}{\int_0^\infty p(R)dR} \qquad \text{(SI-4)}$$

$$p(R)=A\exp\left[\frac{-(R-\bar{R})^2}{2\kappa^2}\right] \qquad \text{(SI-5)}$$

, $\bar{R}$ being the average radius of the spheres. For $S(q)$ we have assumed a hard-sphere Percus-Yevick potential between the spherical microdomains for the sake of simplicity. It is based on the Ornstein-Zernike formulation of the total correlation function of particles in terms of direct pair correlation and indirect correlation.[4] Percus and

Yevick calculated analytically this total correlation function for a short-range hard-sphere potential between the particles.[5] The final expression for $S(q)$ for an effective hard sphere radius R_{hs} and an effective hard sphere volume fraction Φ_{hs} reads as[6, 7]

$$S(q, R_{hs}, \Phi_{hs}) = \frac{1}{1 + 24\Phi_{hs}\left(\frac{G(A)}{A}\right)}$$

$$\begin{aligned} G(A) &= \frac{\alpha}{A^2}(\sin A - A\cos A) + \frac{\beta}{A^3}\left(2A\sin A + \left(2 - A^2\right)\cos A - 2\right) \\ &+ \frac{\gamma}{A^5}\left(-A^4\cos A + 4\left[\left(3A^2 - 6\right)\cos A + \left(A^3 - 6A\right)\sin A + 6\right]\right) \end{aligned} \quad \text{(SI-6)}$$

$$\alpha = \frac{(1 + 2\Phi_{hs})^2}{(1 - \Phi_{hs})^4}, \quad \beta = -6\Phi_{hs}\frac{\left(1 + \frac{\Phi_{hs}}{2}\right)^2}{(1 - \Phi_{hs})^4}, \quad \gamma = \frac{\Phi_{hs}(1 + 2\Phi_{hs})^2}{2(1 - \Phi_{hs})^4},$$

$$A = 2qR_{hs}$$

The scattering intensity of the above mentioned model is compared with scattering curves of S-MAA-8-M/$(C12)_2$/X ($0.1 \leq X \leq 0.5$). Very good agreement between the model and the experimental data is obtained (see Figure 5, a-e, of the paper). The extracted values for the average radius of the (AC-block)-filled spherical microdomains R'_{AC} ($= \bar{R}$ in eqns. SI-4 and SI-5), κ, $R_{hs.}$ and Φ_{hs} are presented in Table SI-1.

Table SI-1.

sample	R'_{AC} (Å)	κ (Å)	R_{hs} [±5 (Å)]	Φ_{hs} (±0.05)
S-MAA-8-M/$(C12)_2$/0.1	68	12	122	0.47
S-MAA-8-M/$(C12)_2$/0.2	69	13	122	0.46
S-MAA-8-M/$(C12)_2$/0.3	72	14	121	0.45
S-MAA-8-M/$(C12)_2$/0.4	80	11	126	0.47
S-MAA-8-M/$(C12)_2$/0.5	74	14	133	0.48

3. Nano-segregated state

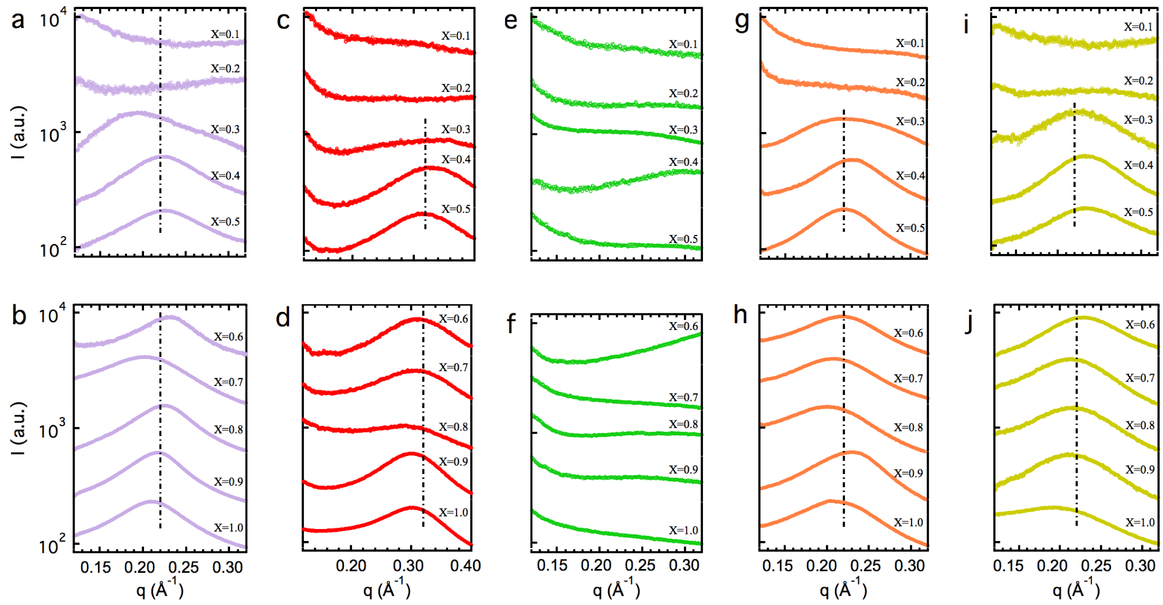

Figure SI-1. SAXS patterns of [(a) and (b)] S-MAA-15/$(C12)_2$/X, [(c) and (d)] S-MAA-15/$(C8)_2$/X, [(e) and (f)] S-MAA-15/$(C8)_4$/X, [(g) and (h)] S-MAA-17-M/$(C12)_2$/X, and [(i) and (j)] S-MAA-8-M/$(C12)_2$/X. In (a)-(d) and (g)-(j) dashed-dotted lines are the approximate positions of the broad peak.

References

1 A. Guinier and G. Fournet, *Small-Angle Scattering of X-rays*, John Wiley & Sons, 1955.

2 J. Ilavsky and P. R. Jemian, *J. Appl. Crystallogr.*, 2009, **42**, 347-353.

3 D. J. Kinning and E. L. Thomas, *Macromolecules*, 1984, **17**, 1712-1718.

4 L. S. Ornstein and F. Zernike, *Proc. Acad. Sci. Amsterdam*, 1914, **17**, 793-806.

5 J. K. Percus and G. J. Yevick, *Physical Review*, 1958, **110**, 1-13.

6 N. W. Ashcroft and J. Lekner, *Phys. Rev.*, 1966, **145**, 83-90.

7 E. W. Kaler, K. E. Bennett, H. T. Davis and L. E. Scriven, *J. Chem. Phys.*, 1983, **79**, 5673-5684.